J. Fluid Mech. (1985), *vol.* 158, *pp.* 137–152
Printed in Great Britain

Simulation of blast waves with tailored explosive charges

By M. SANAI, H. E. LINDBERG† AND J. D. COLTON
SRI International, Menlo Park, California 94025

(Received 20 November 1984)

We have developed a compact and cost-effective shock tube to simulate the static and dynamic pressures of blast waves. The shock tube is open at both ends and is driven by high explosives distributed over a finite length of the tube near one end. The overall charge length is determined by the simulation time of interest, and the charge-density distribution is tailored to produce the pressure-waveform shape desired. For the shock tube to simulate a typical blast wave, the charge density must be highest at the charge front (closest to the test section) and gradually reduced towards the back. The resulting shock tube is an order of magnitude shorter than a conventional dynamic airblast simulator (DABS) in which concentrated explosives are used to drive the shock.

Tailored charges designed using this method were built and tested in a simulation development programme sponsored by the U.S. Defense Nuclear Agency (DNA). The pressures measured for several charge distributions agreed very well with SRI's PUFF hydrocode computations and demonstrated the feasibility of the compact simulator under realistic test conditions.

1. Introduction

Structural loads resulting from nuclear-weapon effects are often simulated by using conventional high explosives. A compact and cost-effective blast-wave simulator can be obtained by distributing and tailoring the charge configuration according to the desired pulse shape. Figure 1 illustrates the application of this concept to dynamic airblast simulators (DABS). Figure 1(*a*) shows a conventional DABS, in which concentrated high explosives are used to drive an airblast down a semicircular shock tube. The driver end is usually blocked by a concrete wall supported by sand. For simulation of low-pressure airblasts (below 5 MPa), the tube has to be quite long (about 350 m for a 3 MPa shock overpressure from a 3 megaton (Mt) nuclear blast) in order that the very high pressures generated by the explosives attenuate to the desired levels. Figure 1(*b*) depicts schematically how shock-tube length may be reduced by uniformly distributing the explosives over a finite length. Figure 1(*c*) shows the even greater reduction obtained by tailoring the charge density so that it is highest at the front end of the explosive driver section (nearest to the test section) and is gradually reduced towards the back. The driver end of the shock tube is left open to eliminate reflection from a closed end. This configuration also reduces cost.

Several aspects of the development of a compact blast wave simulator are discussed here. First, we used the distributed-charge concept to design a compact DABS for simulating the airblast environment associated with a 3 Mt nuclear burst at 3.1 MPa

† Present address: Aptek, Inc., Mountain View, CA 94043.

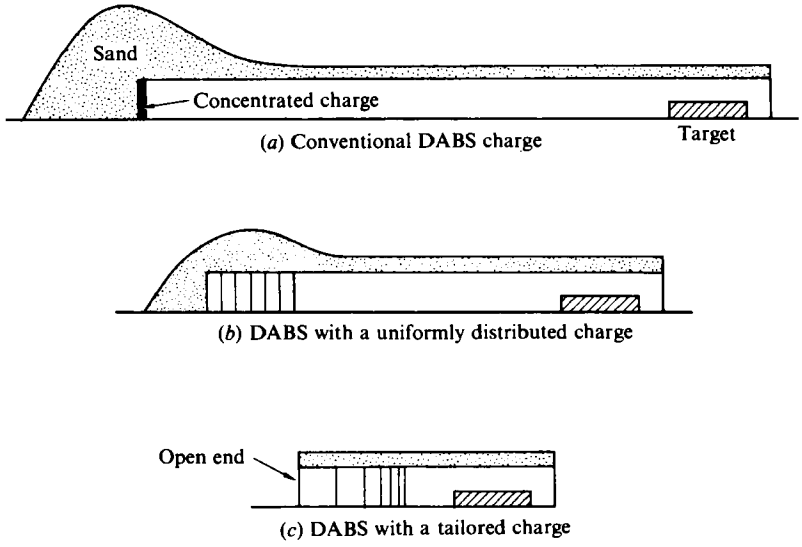

FIGURE 1. Schematic of dynamic airblast simulators (DABS).

pressure range. Then we use the one-dimensional PUFF 8 (Seaman & Curran 1978) Lagrangian computer code to calculate the pressure histories at various locations in the shock tube, and the TIGER code (Cowperthwaite & Zwisler 1973) to study the effect of adding foam to the driver. Finally, we evaluate the performance of the simulator on the basis of several shock-tube experiments in which distributed charges were used.

2. Uniform charge distribution

We first investigate charges with a uniform distribution of the explosives over a finite length by comparing incident-pressure histories from various charge lengths. As a reference, figure 2 shows the pressure histories at 100 m and 200 m for a 0.2 m long solid-explosive charge (280 kg/m^2), detonated instantaneously at time zero. The peak pressure drops and the waveform expands as the shock propagates. The waveform at 100 m (measured from the front surface of the explosive) shows that the rate of change of pressure in air (solid lines in figure 2) differs from that in detonation products (dashed lines in figure 2). This difference becomes less detectable as the shock propagates. In this and all subsequent calculations, the explosive product is modelled as a perfect gas with an initial specific energy e_0 and a constant specific-heat ratio γ. The values of e_0 and γ are inferred from shock-tube experiments similar to those discussed in §4.

The pressure histories obtained from the same amount of explosives (280 kg/m^2) distributed uniformly over a 25 m distance are shown in figure 3. In contrast with the peaked waveforms obtained with the solid explosive charge, a flat-topped waveform with a lower peak pressure is observed at the 100 m standoff location ($x = 125$ m from the closed end of the tube). As the shock propagates, the flat-top portion of the wave is depleted, until at 200 m standoff ($x = 225$ m) the waveform degenerates into a peaked shape similar to that of the reference case (also see the inset in figure 4). The peak pressure obtained with the 25 m charge is 2 MPa, and remains unchanged over the 100 m propagation distance shown in figure 3. This is a

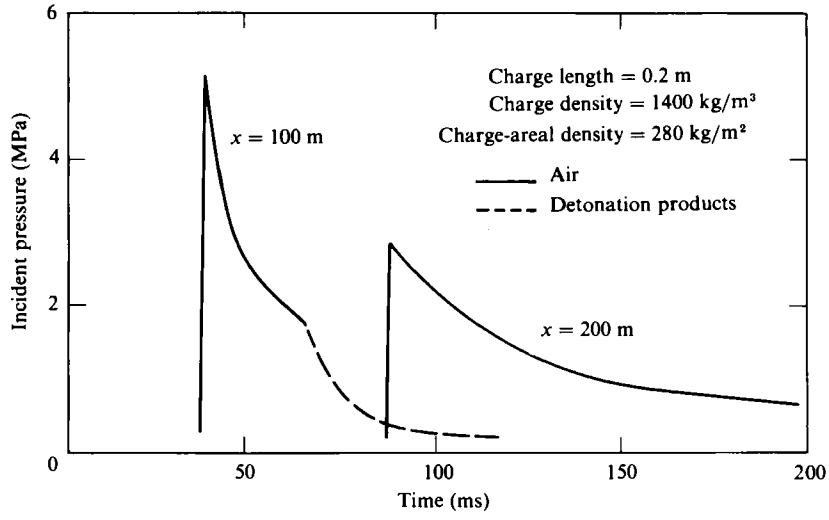

FIGURE 2. Incident-pressure histories at 100 and 200 m for a 0.2 m concentrated charge at the closed end of the shock tube.

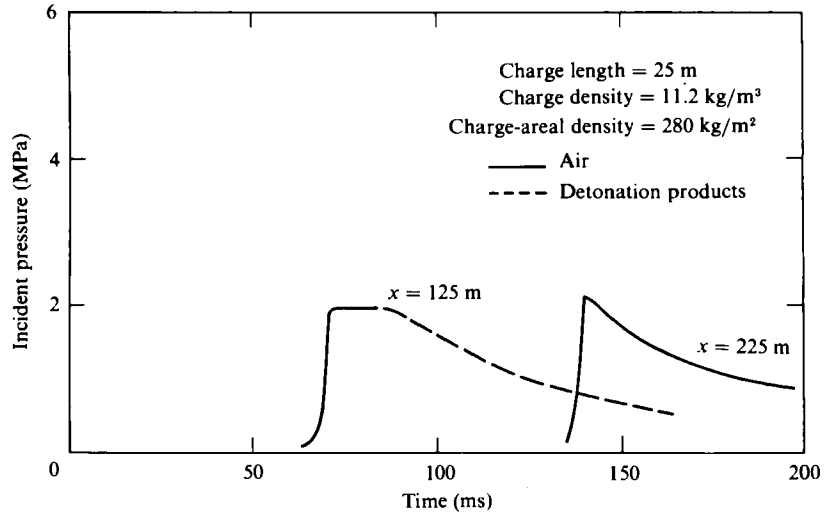

FIGURE 3. Incident-pressure histories at 125 and 225 m for a 25 m uniformly distributed charge.

characteristic feature of shocks driven by a finite-length, constant driver pressure. When the rarefaction from the rear of the driver section reaches the shock, the waveform ceases being flat-topped; during further propagation the peak pressure decays.

To investigate the effect of the charge length, we performed similar calculations for 12.5 and 75 m uniform explosive charges. Figure 4 shows the variation of peak pressure with distance for the four charge lengths considered. For the reference solid explosive charge (dashed line in figure 4) a continuous attenuation of the peak pressure is observed. For other cases the peak pressure does not attenuate as long as the waveform has a flat top similar to that seen in figure 3. The point at which the peak pressure starts to decrease occurs at a distance of about 10 charge lengths.

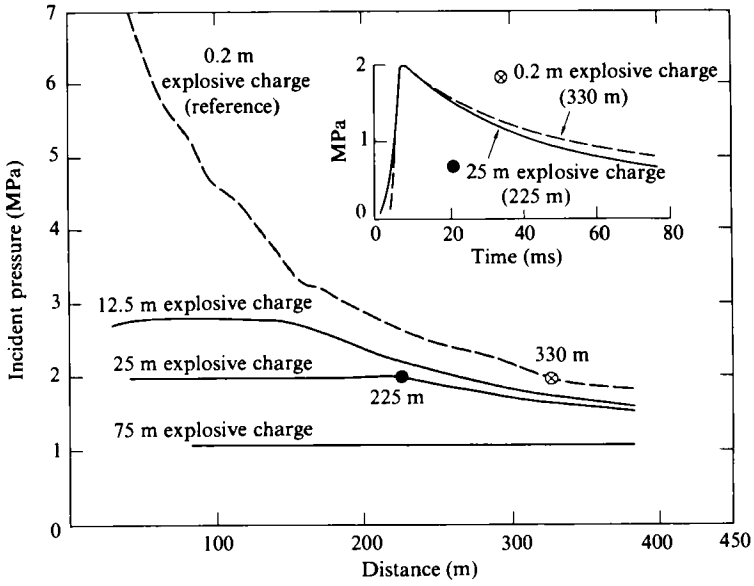

FIGURE 4. Variation of incident peak pressure versus range for the 0.2, 12.5, 25 and 75 m uniformly distributed explosive charges; the inset shows the similarity of pressure waveforms for equal peak pressure.

This point represents the minimum standoff required for generating a peaked waveform. The minimum standoff depends on the shock strength and generally decreases as the charge density increases (also see figure 4).

We now compare the pressure histories to estimate the extent to which the shock-tube length may be reduced by using a uniformly distributed charge. The inset in figure 4 shows that the pressure waveform obtained from the 25 m charge at 225 m is essentially identical with that obtained from the reference concentrated charge at 330 m. This represents a reduction of 105 m (or 32 %) in shock-tube length for a 2 MPa peak pressure. A similar comparison for the 12.5 m charge (not shown here) indicates a 31 % reduction in tube length for a 2.8 MPa peak pressure. Therefore a 30 % reduction in shock-tube length can be obtained by uniformly distributing the charge in the driver.

3. Tailored charge distribution

The formation of a desired waveform may be expedited by tailoring the charge according to the shape of that waveform. Figure 5 shows the density distribution in a charge tailored to produce a peaked waveform close to the charge. The charge is divided into zones of lengths l_i and constant charge densities ρ_i. The charge density is largest at the front (nearest to the test section), and is gradually reduced toward the back. The driver end of the shock tube is left open to eliminate shock reflections from a closed end.

The qualitative relationships between the parameters that characterize a tailored charge (overall charge length L, zone widths l_i and zone charge densities ρ_i) and those that characterize an exponential-like pulse (peak pressure P_s and pulse duration T) are given in figure 5. The charge density ρ_5 in the front zone determines the shock pressure, and the width l_5 of the front zone determines the minimum standoff at which

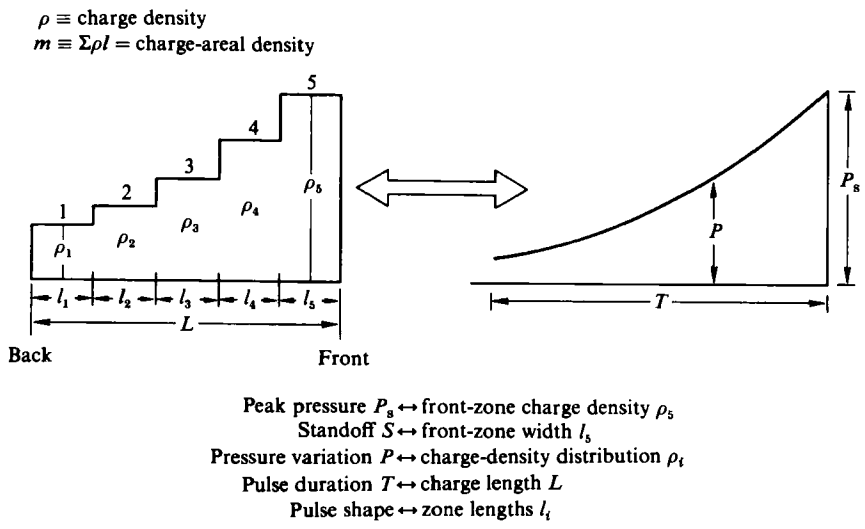

FIGURE 5. Representation of a tapered charge and the resulting pressure waveform.

a peaked waveform occurs. The total charge length is approximately proportional to the resulting pulse duration, and the distribution of the charge density, defined by l_i, determines the waveform. To match a given waveform, the spatial variation of the charge density in the explosives must match the temporal variation of the pressure waveform.

3.1. *Example of a compact blast-wave simulator*

As a typical application of the tailored-charge concept, we have designed, with the aid of the PUFF code, a charge for simulating the flow environment that results from a 3 Mt yield nuclear burst at the 3.1 MPa pressure range. Figures 6 and 7 show the charge configuration and the resulting pressure and impulse histories at a 24 m standoff. The charge consists of 5 zones and is 40 m long. The charge density and width of the first zone are adjusted to produce the 3.1 MPa peak pressure at the selected standoff of 24 m. The pressure drops in distinct steps. Each step represents a local constant-pressure region, and the steps on the waveforms correspond one-to-one with the zones in the tailored charge. The flatness of the steps is exaggerated here because the PUFF code does not account for the mixing of the explosive products from adjacent zones. If desired, the waveform can also be made smoother by increasing the number of zones. With an infinite number of zones, the waveform becomes perfectly smooth, corresponding to a smooth variation in charge density.

Comparisons of the calculated and reference pressure and impulse histories (dashed lines in figures 6 and 7) indicate that the present simulator provides a satisfactory match for both static and dynamic pressures. Use of a variable γ in the equation of state for the explosive products is believed to give a better stagnation-pressure match than that seen in figure 7 (discussed in §4). We conclude that the present simulator can replace the conventional DABS (figure 1*a*) for testing structures in blast-wave environments, even though the working gas consists mainly of explosive products rather than air.

The variation of peak pressure and impulse over the test section of a blast-wave simulator must also be considered. The solid lines in figure 8 show the variation with distance of the incident peak pressure, incident impulse to 80 ms after shock-arrival

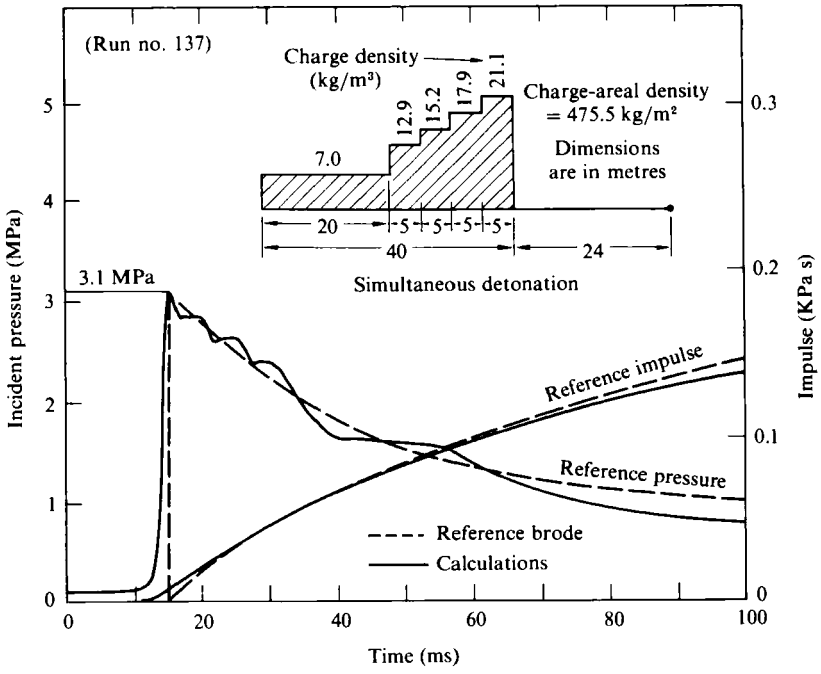

FIGURE 6. Incident-pressure and impulse histories at 25 m standoff for a 40 m tapered charge compared with reference values.

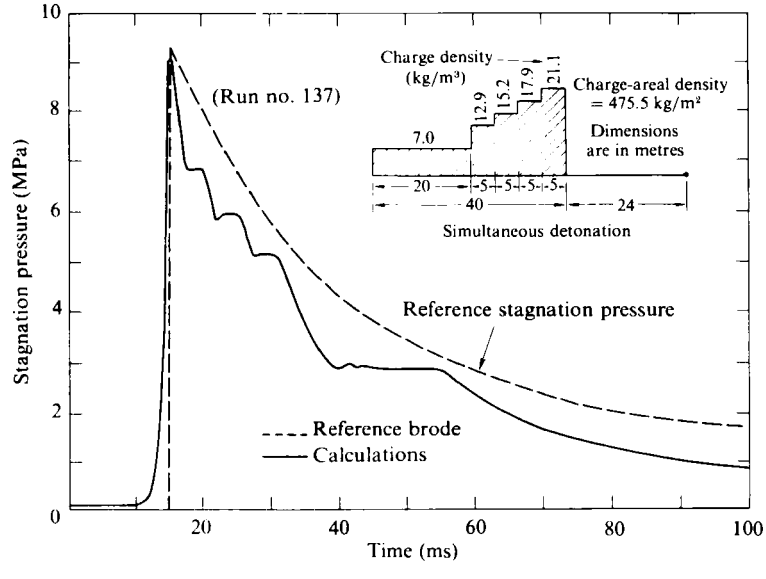

FIGURE 7. Stagnation-pressure histories at 24 m standoff for a 40 m tapered charge compared with reference values.

time, and peak stagnation pressure for the 40 m tailored charge shown in figures 6 and 7. Also shown (as dashed lines) are the corresponding reference values for the pressures and impulse. The overall attenuations in the peak pressures are essentially the same for the tailored charge and the reference case. However, the attenuation occurs in shallow steps for the tailored charge, in contrast with the smooth drop in

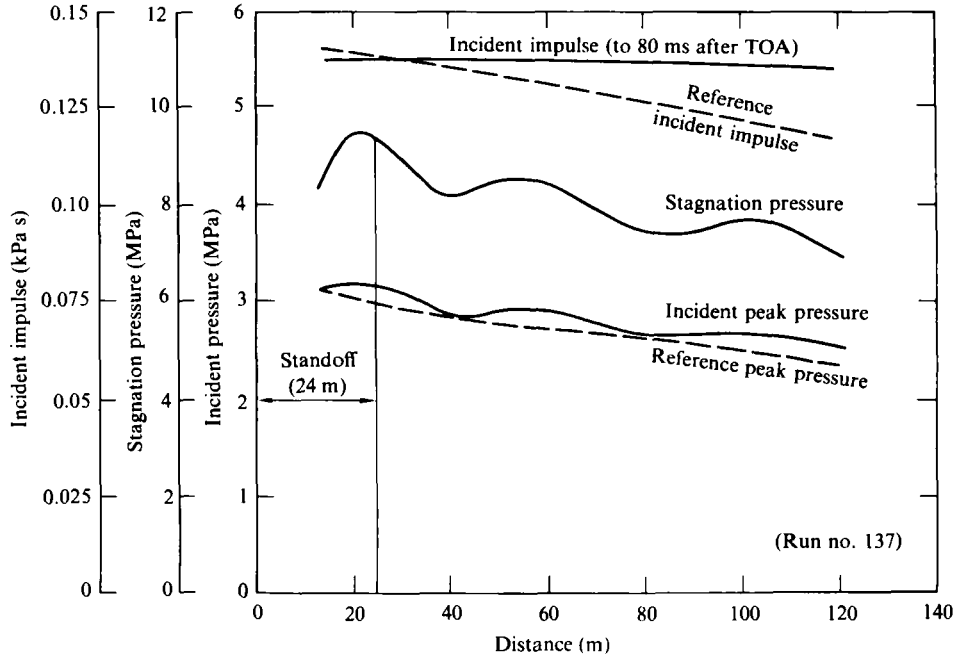

FIGURE 8. Variation of incidence pressure and impulse and stagnation pressure with distance compared with reference values.

the reference case. This is consistent with the steplike pressure waveforms that result from the tailored charges. As noted, mixing, which was not addressed in our calculations, would tend to smooth these steps. If desired, the attenuation may be made smoother by increasing the number of zones in the tailored charge. In contrast with the decaying impulse in the reference case, the impulse from the tailored charge is essentially constant. This limits the accuracy of the simulation for a long, impulse-sensitive target.

3.2. *Effect of running detonation*

In the calculations presented thus far, we have assumed an instantaneous detonation of all the explosives at time zero. In actual experiments the detonation progresses from the initiation point at a finite rate. Figure 9 shows the effect of the detonation initiation point for a 60 m tailored charge. The three cases shown correspond to simultaneous detonation (figure 9*a*), detonation initiated at the front end and running upstream at 2000 m/s (figure 9*b*), and detonation initiated at the back end and running downstream at 2000 m/s (figure 9*c*). The simultaneous-detonation case is obtained by assuming a very high detonation velocity (10^8 m/s in figure 9*a*), resulting in a pressure history that is independent of the detonation velocity or initiation point. Comparisons of the pressure histories indicate that both the peak pressure and pulse durations are influenced by the detonation initiation point. For the back-end detonation the peak pressure is increased by 70 %; the pulse duration, as measured by the width at half peak pressure, is reduced by 50 % compared with the simultaneous-detonation case. Back-end detonation is therefore undesirable because a longer charge and therefore a longer shock tube will be required to produce the same pulse duration. For the front-end detonation the peak pressure is reduced by 17 %, and the pulse duration is increased by 50 % compared with the simultaneous-

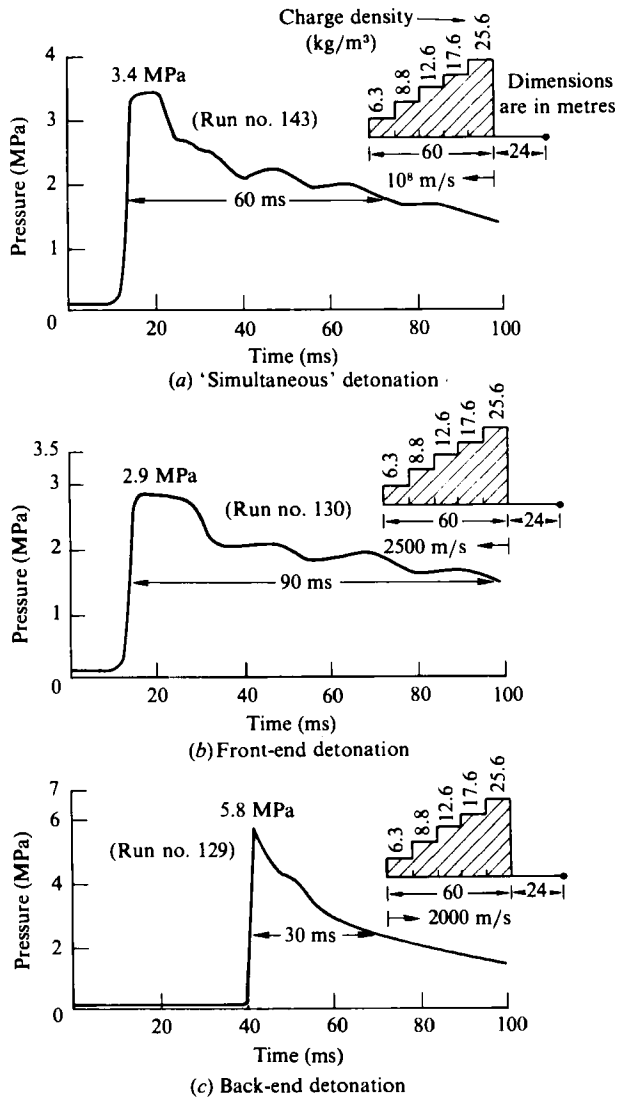

FIGURE 9. Incident-pressure histories showing the effect of the detonation-initiation point (24 m standoff, 850.8 kg/m² charge-areal density).

detonation case. Thus front-end detonation is preferable because it minimizes the required charge length.

We performed calculations for a 20 m tailored charge and front-end initiation to determine the results of the effective detonation velocity. Figure 10 shows the pressure histories for a simultaneous detonation and detonation velocities of 4000, 2000 and 1000 m/s. The trends observed indicate that the pulse width increases and that the peak pressure decreases as the detonation velocity is lowered. Table 1 summarizes the peak pressures and pulse widths for various detonation velocities and indicates that for a detonation velocity of 4000 m/s, which is typical of slurry explosives such as Iremite 60,† the pulse duration is increased by 20.8% compared with a simultaneous detonation. Lowering the detonation velocity to 2000 m/s (e.g.

† Iremite 60 is a commercial explosive manufactured by IRECO, Salt Lake City, Utah.

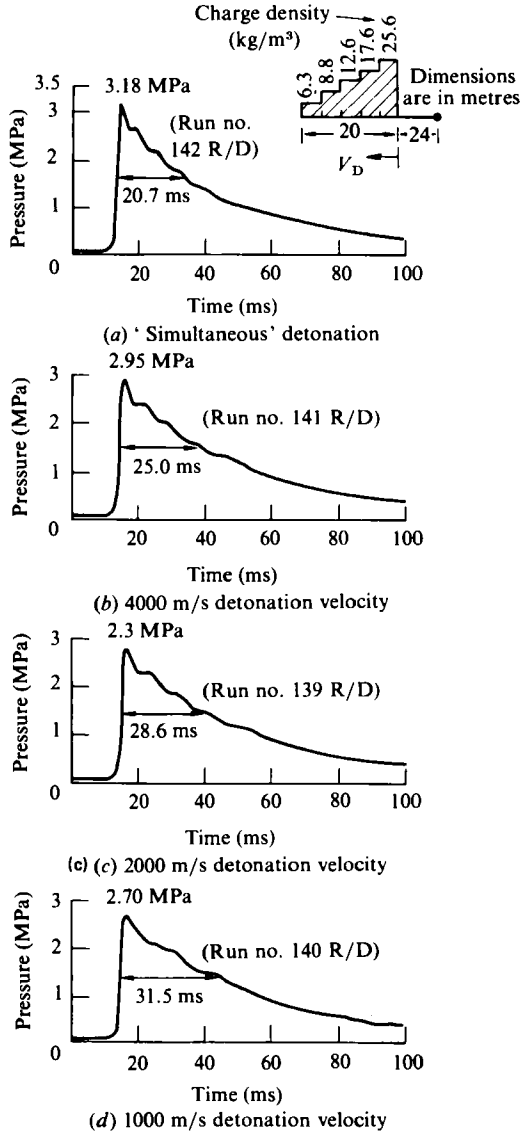

FIGURE 10. Incident-pressure histories showing the effect of detonation velocity V_D on pulse width (24 m standoff, 283.6 kg/m² charge-areal density).

by using a coiled explosive) would increase the pulse duration by another 14%. Reducing detonation velocity to 1000 m/s or less (shown by daggers in table 1) is believed to be impracticable because the air shock generated by the detonation moves ahead of the detonation front and may disintegrate the charge or cause a premature detonation.

3.3. *Use of plastic foam in the driver*

A method that may further reduce the shock-tube length consists of placing more plastic foam in the driver than would ordinarily be used for structural support of the explosive conventional DABS. We have investigated the addition of foam to an explosive charge made from Iremite 60 explosives in two successive steps: First, by

Run number	Detonation velocity V_D (m/s)	Peak pressure		Pulse width at half peak pressure	
		MPa	% change	ms	% change
142	10^8	3.18	0	20.7	0
141	4000	2.95	−7.2	25.0	+20.8
139	2000	2.80	−11.9	28.6	+38.2
140†	1000†	2.70†	−15.1†	31.5†	+52.2†

† Impracticable because the shock wave generated by detonation moves ahead of the detonation front

TABLE 1. Effect of detonation velocity on incident peak pressure and pulse duration

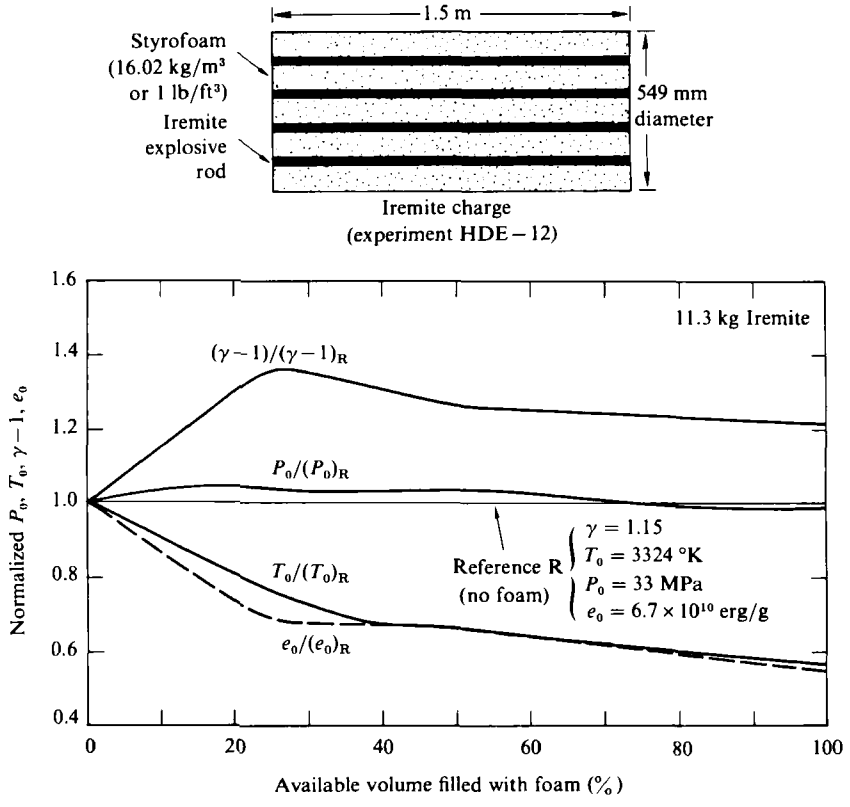

FIGURE 11. Equilibrium pressure P_0, temperature T_0, internal energy e_0 and gas constant $\gamma-1$ for various amounts of foam used in a 11.3 kg Iremite charge (1.5 m uniformly distributed charge).

using the TIGER code we calculated the equilibrium thermodynamic properties of various mixtures of Iremite 60 explosive and foam after detonation at constant volume. Those results were then used as input to the PUFF code for calculating the pressure histories.

Thermodynamic properties of the detonation products calculated with TIGER are plotted in figure 11 for various amounts of a 16.02 kg/cm³ styrofoam placed in the shock-tube driver of a typical experiment (these experiments are discussed in more

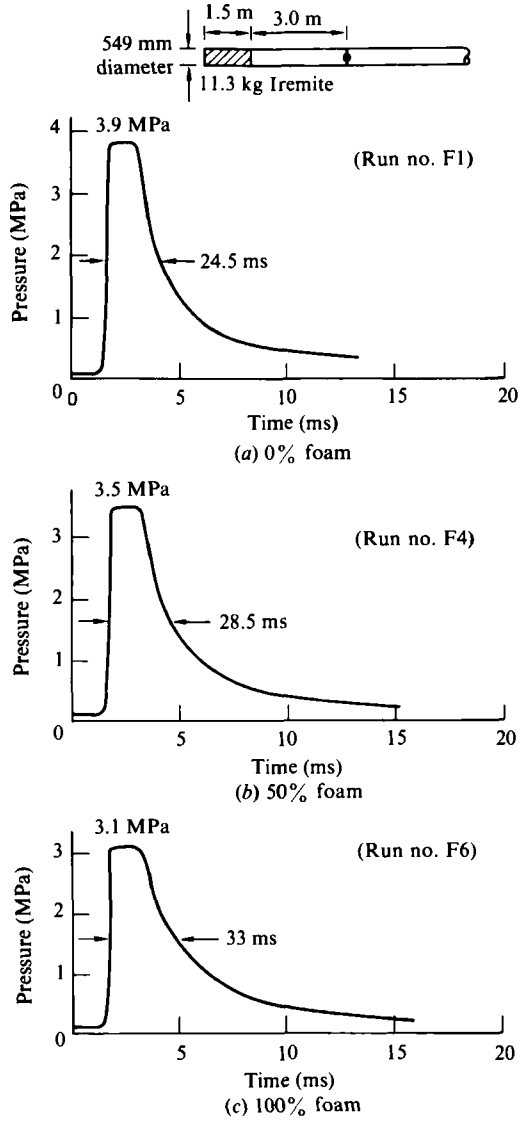

FIGURE 12. Incident pressure histories for various amounts of foam used in a 11.3 kg Iremite charge (1.5 m uniformly distributed charge, 3 m standoff).

detail in §4). The driver section is 1.5 m long and 549 mm in diameter and contains 11.3 kg of Iremite explosives uniformly distributed over the length. Pressure P, temperature T, specific energy e_0 and specific-heat ratio γ of the detonation products are normalized relative to the case of pure explosives for which no foam is used. The temperature and specific energy decrease monotonically with increased amounts of foam. The specific-heat ratio function $\gamma - 1$ passes through a maximum at about 25% foam, which coincides with the temperature at which solid materials (aluminium oxide and carbon) appear in the detonation products (Sanai 1985 in preparation). All thermodynamic properties are found to be sensitive to the presence of foam, except for the detonation pressure, which remains essentially constant at 33 MPa. Thus the detonation pressure in the DABS driver is primarily determined by the charge

Run number	% foam	Peak pressure MPa	Peak pressure % change	Pulse width at half peak pressure ms	Pulse width at half peak pressure % change
F1	0	3.9	0	24.5	0
F2	11.5	3.8	−2.6	25.0	+2.0
F3	25	2.6	−7.7	25.5	+4.1
F4	50	3.5	−10.3	28.5	+16.3
F5	75	3.3	−15.4	30.5	+24.5
F6	100	3.1	−20.5	33.0	+34.7

TABLE 2. Effect of foam density on incident peak pressure and pulse duration

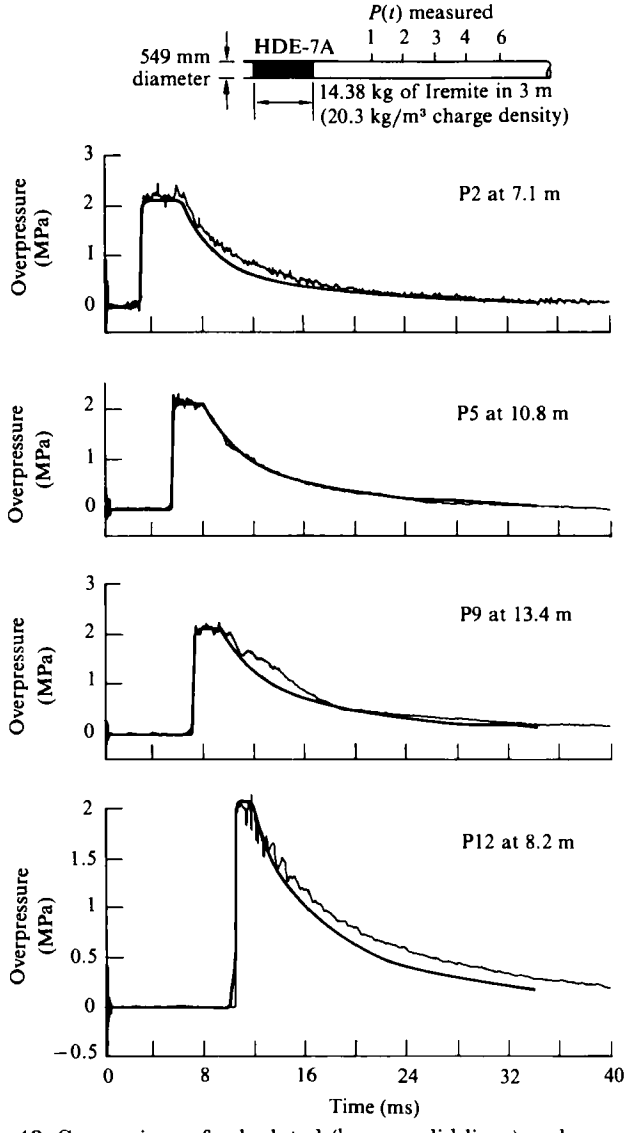

FIGURE 13. Comparison of calculated (heavy solid lines) and measured incident overpressure histories at four locations in experiment HDE-7A.

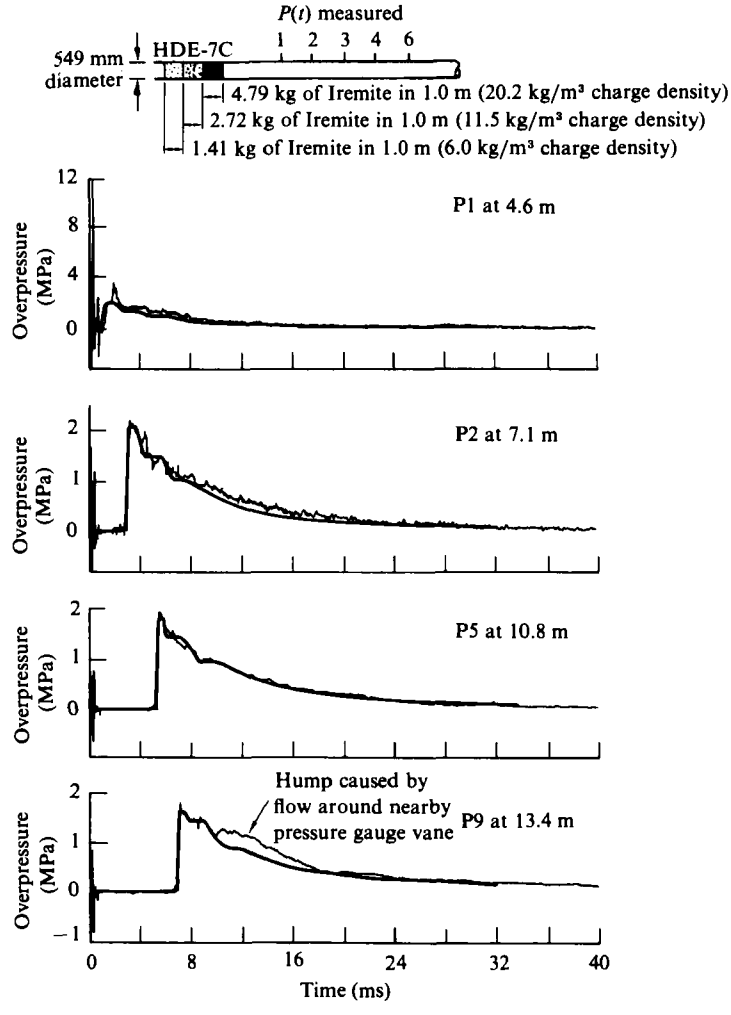

FIGURE 14. Comparison of calculated (heavy solid lines) and measured incident overpressure histories at four locations in experiment HDE-7C.

density, and the addition of foam does not substantially alter the resulting pressure.

We now use the PUFF code to calculate the pressure histories for different amounts of foam in the driver. Figure 12 shows the pressure histories for three cases in which 0, 50 and 100 % of the available volume of the charge is filled with the 16.02 kg/m^3 foam. The trend observed in figure 12 is that the foam reduces the peak pressure and widens the waveform. As the amount of foam is increased from 0 to 100 %, the peak pressure is reduced from 3.9 to 3.1 MPa, and the pulse width at half the peak pressure is increased from 24.5 to 33 ms. The relative changes in peak pressures and pulse widths are tabulated in table 2 for various amounts of foam. The largest decrease in peak pressure is 20.5 % and the largest increase in pulse width is 34.7 % – both of which are obtained for a case in which the driver is fully packed with foam. It appears likely that for this case full decomposition of foam would not occur in actual experiments. Assuming that 50 % foam is the limit for complete foam composition, we infer from the data presented in table 2 that a 16 % reduction in shock-tube length is possible by adding foam to the driver.

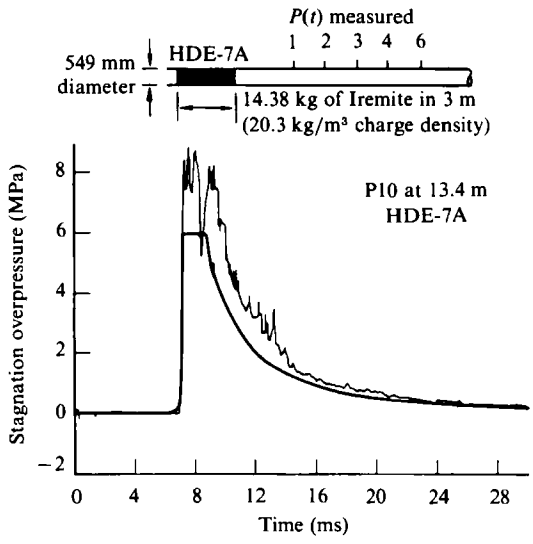

FIGURE 15. Comparison of calculated (heavy solid lines) and measured stagnation overpressure histories at 13.4 m for experiment HDE-7A.

4. Comparison with experimental results

Encouraged by the results of the foregoing calculations, the U.S. Air Force asked the New Mexico Research Institute (NMERI 1981) to test the tailored-charge concept by performing several shock-tube experiments. Figure 13 shows the calculated and measured pressure histories resulting from a 3 m uniformly distributed charge placed in an open-ended 560 mm diameter shock tube. PUFF calculations (shown as heavy solid lines in figure 13) match the experimental results very well. The waveform has a flat top that persists even to the last measurement location (P12 at 8.2 m), and, as predicted by the theory, the peak pressure remains unchanged over the entire propagation distance.

Figure 14 shows the calculated and measured pressure histories for a tailored charge consisting of three 1 m zones. The charge density of the front zone is the same as the 3 m uniform charge (figure 13), and drops to about 30 % of the front value at the open end of the driver. The PUFF calculations (heavy solid lines) again match the experimental results very well. In contrast with the uniformly distributed charge, a peaked waveform is obtained from the tailored charge at a standoff of less than two charge lengths. The pressure histories at the 7.1 m location (standoff of about 1.5 times the charge length) have a peak pressure of 2.1 MPa for both the tailored charge (figure 14) and the uniformly distributed charge (figure 13). However, the waveform from the tailored charge is peaked, whereas the one for the uniform charge is flat-topped. This difference supports our conclusion that the formation of a peaked waveform is expedited when a tailored charge is used.

Figure 15 compares between calculated (heavy solid lines) and measured stagnation-pressure histories at 13.4 m for the 3 m uniform charge. The overall shapes of the waveforms agree reasonably well, but the calculated peak stagnation pressure is about 25 % lower than the measured value. This difference may result from the manifestation of real-gas effects at the shock front. Using a specific-heat ratio of 1.25 for shocked air, rather than the value of 1.4 used in the present calculations, results in a 30 % increase in the calculated peak stagnation pressures but does not change the

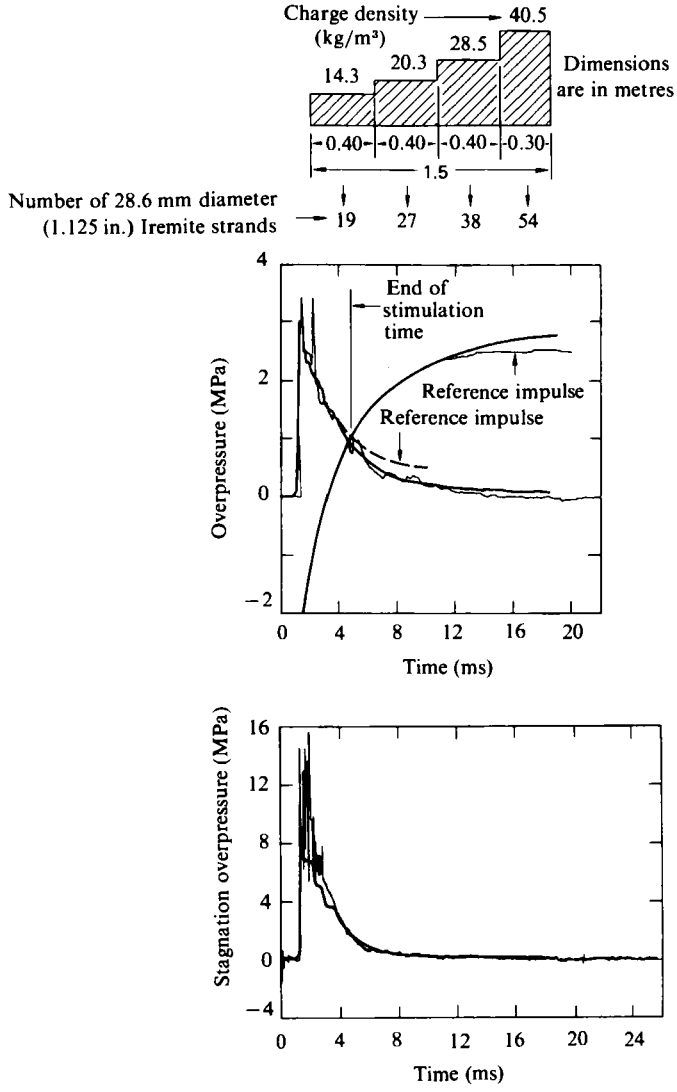

FIGURE 16. Comparison of calculated (heavy solid lines) and measured overpressure and impulse histories at the desired test point (2 m standoff) in hybrid-21 calibration experiment.

calculated peak pressures by more than 5 %. Therefore we believe that the prediction of the stagnation pressures may be improved by using an equation of state that accounts for the variable value of γ for shocked air.

Using the values of specific energy and specific heat ratio obtained from matching the above experimental results ($e_0 = 4.7 \times 10^{10}$ erg/g, $\gamma = 1.20$), we designed a tailored charge for the U.S. Air Force Weapons Laboratory (AFWL) Hybrid-21 experiment in which a $\frac{1}{21}$ scale model of a shelter was loaded by a combination of a DABS and a high-explosive simulation technique (HEST) (Palmer 1981). Results from the DABS calibration experiment (in the absence of the physical model) are shown in figure 16. The 1.5 m long charge consisted of 28.6 mm diameter Iremite 60 explosive strands suspended parallel to the shock-tube axis. The shock tube was constructed from a steel plate rolled into a 1.83 m diameter semicircle. The charge had four zones, and the width and charge density of the front zone were adjusted

to produce the desired pressure at a 2 m standoff. The pretest calculations (the heavy solid lines in figure 16) and the reference pressure (the dashed lines) agree very well with the measured pressure history up to the desired simulation time of 3.8 ms (80 ms full-scale). We believe that the spike that appears at about 2.1 ms on the measured pressure history results from lateral reverberation of oblique shocks generated in the driver section. Using more (but thinner) explosive strands placed closer to each other should help eliminate this problem.

5. Conclusion

The calculations and experimental results presented here demonstrate that the length of a conventional DABS used to simulate the environments associated with blast waves can be reduced by nearly an order of magnitude when the charge is tailored according to the shape of the desired waveform. Shortening the tube length and removing the driver endwall are expected to lower construction costs significantly without compromising the quality of the resulting flow environment.

The concept of matching the charge configuration with the desired pulse is equally applicable to complex waveforms in which more than one peak is present. In this case, tailored charges would be spaced and detonated at appropriate times to generate the desired multipeak pressure waveform. The rules discussed for designing tailored charges are also applicable to each of the multiple charges.

The work described here was supported by the U.S. Defense Nuclear Agency under Contract DNA001-80-C-0272 and was monitored by Major M. E. Furbee. Experiments were performed by NMERI under contract to AFWL, Albuquerque, New Mexico. We acknowledge the efforts of L. Seaman from SRI, who is responsible for the development of the SRI version of the PUFF code. He added several options to the code for use in the present calculation. PUFF and TIGER code calculations were performed by J. Kempf and B. Lew. We are particularly indebted to R. Port and H. Brode of Research and Development Associates, Marina Del Rey, California, who encouraged us to pursue methods for decreasing DABS costs.

REFERENCES

COWPERTHWAITE, M. & ZWISLER, W. H. 1973 TIGER program documentation. *STI Publ.* 2106.

NMERI 1981 Data report on hybrid driver evaluation tests. *New Mexico Research Institute, Albuquerque.*

PALMER, D. G. 1981 HBRD-1(21) final data report. *Rep.* NMERI-TA-9-14, *New Mexico Research Institute, Albuquerque.*

SANAI, M. 1985 Development of a compact dynamic airblast simulator (DABS) for proof tests of MX shelter models. *Final Rep. SRI Project* PYU-1596 (to appear).

SEAMAN, L. & CURRAN, D. R. 1978 SRI PUFF 8 computer program for one-dimensional stress wave propagation. *Final Rep. SRI Project* PYU-6802.